Proceedings of the 2nd Winter Workshop S&SRES'96, Polanica Zdrój 1996

ENERGY TRANSFER TO TRACE IMPURITIES IN $Cs_2NaY_{1-x}Pr_xCl_6$: CONSEQUENCES FOR INTERPRETATION OF EMISSION DECAY CURVES

S.O. VASQUEZ

Department of Basic Chemistry, Faculty of Physical and Mathematical Sciences
University of Chile
Tupper 2069, P.O. Box 2777, Santiago, Chile

AND C.D. FLINT

Laser Laboratory, Department of Chemistry, Birkbeck College, University of London
Gordon House, 29 Gordon Square, London WC1H 0PP, United Kingdom

We report the $^3P_0 \rightarrow {}^3H_4$ and $^3P_0 \rightarrow {}^3H_4$ luminescence decay curves of $Cs_2NaY_{1-x}Pr_xCl_6$ at 20 K as a function of excitation wave number in the region of the transitions to the $^3P_0$ state near 20 602 cm^{-1}, the $^3P_1$ state near 21 200 cm^{-1} and the six components of the $^1I_6$ state distributed over the region 21 164 to about 22 000 cm^{-1}. For $x = 0.001$ and excitation into the absorption maxima, the decay curves are independent of excitation wave number and of the emission transition monitored, and are exactly exponential. Excitation at regions of weak absorption between the main absorption bands produces markedly different decay curves characterised by a prominent very fast relaxation at short times and a long exponential tail. The fast decay is strongly non-exponential. On increasing the temperature, this fast process becomes less prominent, and it is not detectable in the 298 K curves. For $x \geq 0.05$ the fast process is not present at any temperature. We propose that this fast process is due to emission from $PrCl_6^{3-}$ ions perturbed by a nearby water molecule.

PACS numbers: 13.40.Hq, 31.70.Hq, 61.72.Ss, 78.55.Hx

1. Introduction

In a recent series of papers [1–5] we have proposed a simple shell model which may be used to interpret the luminescence decay curves of lanthanide ions undergoing cross-relaxation in high symmetry crystals and applied the model to the cubic lanthanide hexachloroelpasolites $Cs_2NaY_{1-x}La_xCl_6$ where Ln is a trivalent lanthanide ion whose relaxation is responsible for the emission. A feature of this model is that, if the exactly exponential decay curves can be measured for

$x = 1$ and also for a sufficiently dilute crystal that cross-relaxation is negligible, then the non-exponential decay curves obtained at other values of x may be calculated explicitly. Comparison with experimental data (without curve fitting) may then provide evidence for processes which are not included within the simple shell model. Processes which have been considered are local deviations from a uniform distribution of acceptors [2], non-spherical permittivity between the donors and acceptors [5], higher order electric and magnetic multipole coupling [5] and migration amongst the donors [4].

If the shell model is to be used correctly, it is necessary for experimental uncertainties to be reduced to a minimum. In this paper we report the effect of traces of impurities on the luminescence decay curves of $Cs_2NaY_{1-x}Pr_xCl_6$.

2. Cross-relaxation from the $^3P_0$ state of $PrCl_6^{3-}$

The structure of Cs_2NaYCl_6 and $Cs_2NaPrCl_6$ and their mixed crystals has been discussed previously [1]. The $PrCl_6^{3-}$ ions occupy sites of O_h symmetry so that the emission and absorption spectra consist of sharp magnetic dipole origins (where allowed) and broader electric dipole vibronic transitions. The one-phonon spectrum extends to about 290 cm^{-1} with maxima in the one-phonon density of states at 240–276 (ν_3), 98–120 (ν_4) and 70–85 cm^{-1} (ν_6). The ground electronic state is $^3H_4$ with crystal field components at Γ_1, 0; Γ_4, 236; Γ_3, 422 and Γ_5, 701 cm^{-1}. The emissive state in the blue region at low temperatures is the $^3P_0$ at 20 602 cm^{-1}. To high energy of the $^3P_0$ state, the $^3P_1$ is at near 21 200 cm^{-1} and the components of the $^1I_6$ occur between 21 164 and 22 000 cm^{-1} (Ref. [6]).

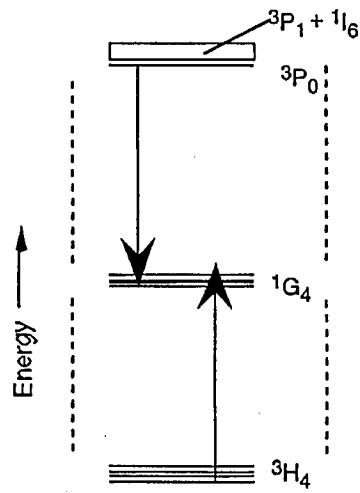

Fig. 1. Simplified energy level diagram for $PrCl_6^{3-}$ showing the cross-relaxation processes considered in this paper. The $^3H_5$, $^3H_6$, ^3F_J and $^1D_2$ energy levels in the region 1000–9000 and near 16 000 cm^{-1} have been omitted for clarity.

The emission from the $^3P_0$ state of $Cs_2NaY_{0.999}Pr_{0.001}Cl_6$ is relatively intense at all temperatures between 18 K and 293 K. The emission from the same state of $Cs_2NaPrCl_6$ is much weaker even at low temperatures and is very weak at room temperature. The luminescence lifetimes decrease by more than 2 orders of magnitude over this concentration range. Clearly a cross-relaxation is involved and the various possibilities at low temperatures have been discussed previously [1]. The only possible cross-relaxations are those involving the $^1G_4$ state with crystal field components at Γ_1, 9853; Γ_3, (not observed, expected position *ca.* 9870) and Γ_4, 9900; Γ_5, 10325 cm^{-1}. The donor pathway is likely to be $^3P_0 \rightarrow {}^1G_4\ (\Gamma_5, \Gamma_4) + \Delta E_{vib}$ and the acceptor process will be $^3H_4 \rightarrow {}^1G_4\ (\Gamma_1, \Gamma_3, \Gamma_4, \Gamma_5) + \Delta E_{vib}$ (Fig. 1). The remaining levels are not involved in the processes discussed in this paper but are given in Ref. [6].

3. Experimental

Large clear, clear colourless single crystals of $Cs_2NaY_{1-x}Pr_xCl_6$ were grown by the Bridgman method and stored as previously described [1]. The samples were cooled using a Oxford CF100 Helium cryostat or a laboratory built nitrogen cryostat.

Measurements of luminescence decay curves were carried out using a Spectron tripled Nd:YAG laser pumping a Spectron dye laser with coumarin 460 as the laser dye (pulse duration 7 ns; up to 30 mJ per pulse; 10 pulses s^{-1}). The emission was measured with a cooled C31034A photomultiplier tube. Samples were studied over a temperature range of 20 K to 300 K, for six excitation wave numbers in the region 20600–22300 cm^{-1} and observing at both 15295 cm^{-1} and 20113 cm^{-1} corresponding to the strong features of the $^3P_0 \rightarrow {}^3F_2$ and $^3P_0 \rightarrow {}^3H_4$ vibronic transitions observed in the luminescence spectra. The output from the photomultiplier was amplified by Stanford Research Systems SR455S preamplifier and the photons counted by a SR430 multichannel scaler/averager. Measurements were carried out on several crystals of each composition.

Excitation spectra were obtained passing the output from the photomultiplier to a boxcar integrator. For all the measurements, the gate width used was 500 μs opening 100 μs after the laser pulse. The excitation wave numbers were scanned between 20600 and 22320 cm^{-1} and observed at both 15295 and 20113 cm^{-1}.

4. Results

Figure 2 shows the 20 K excitation spectra of an $x = 0.01$ sample, the spectrum for the $x = 0.001$ material was similar but gave a weaker signal, especially at the extrema of the dye tuning range. The spectra are in very good agreement with the absorption data [6]. Three *LSJ* terms are expected in this region, $^3P_0$, $^3P_1$ and the six components of $^1I_6$. Detailed assignments of the spectra to individual *LSJ* terms are not available and to some extent meaningless. The important point in the present context is that there are no separations between electronic states of more than three vibrational quanta in the region between the $^3P_0$ and the limit of our excitation experiments at 22300 cm^{-1}, so that relaxation to the $^3P_0$

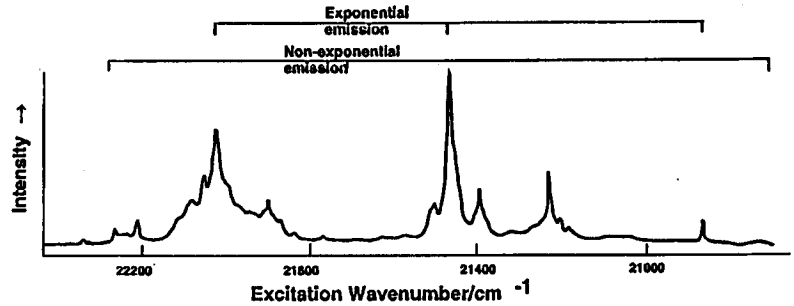

Fig. 2. 20 K excitation spectrum of $Cs_2NaY_{0.99}Pr_{0.01}Cl_6$. Observation wave number 20 113 cm^{-1}. Observation gate 500 μs opening 100 μs after the laser pulse.

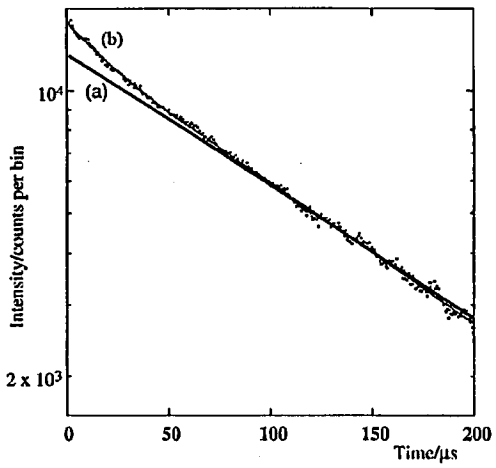

Fig. 3. Initial part of the luminescence decay curve of $Cs_2NaY_{0.99}Pr_{0.01}Cl_6$ at 20 K. Line *a* shows the best single exponential fit, curve *b* the double exponential fit to $I(t) = I(0)[\exp(-7500t) + 0.12\exp(-70000t)]$.

state is expected to be fast at low temperatures. At room temperature, the excitation spectra show only three broad overlapping peaks; due to the usual thermal broadening and perhaps also as a consequence of thermal population of the $^3H_5$ levels.

At 20 K the decay curves of the $^3P_0 \rightarrow {}^3F_2$ and $^3P_0 \rightarrow {}^3H_4$ emission for the $x = 0.01$ material were exactly exponential with a decay constant of 2170 cm^{-1}, and were independent of excitation wave number throughout the region 20 600 to 22 300 cm^{-1}. At higher temperatures there is a detectable contribution from a faster process at short times (Fig. 3). This faster process is present with comparable relative intensity at all excitation wave numbers. The 298 K data are well modelled by a double exponential decay with the smaller decay constant of 7500 s^{-1} and

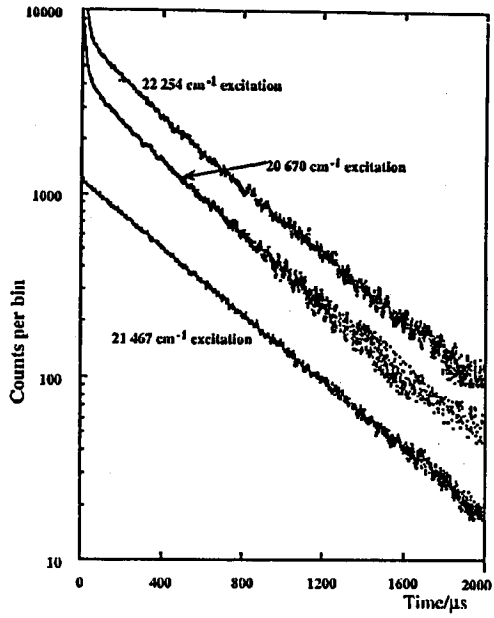

Fig. 4. $^3P_0$ emission decay curves of $Cs_2NaY_{0.99}Pr_{0.01}Cl_6$ at 20 K for three different excitation wave numbers.

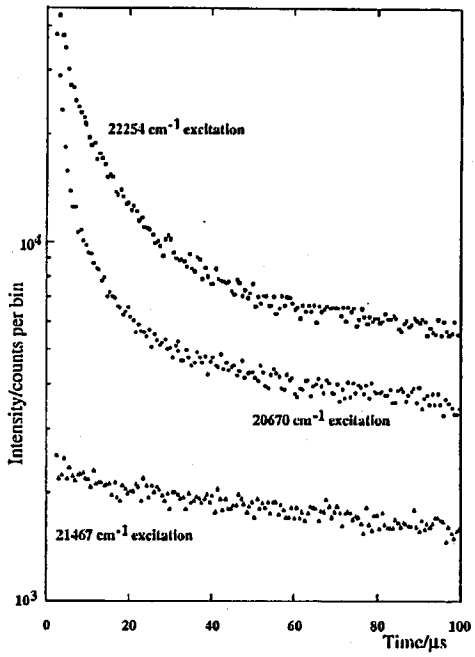

Fig. 5. The inital part of the decay curves shown in Fig. 4.

the larger decay constant of 70 000 cm^{-1}. The ratio of the pre-exponential factors is 0.12. The error in these values for the faster process is rather large since this process only contributes about 1.5% of the emitted photons.

Excitation of the $x = 0.001$ material into the stronger vibronic bands in the region 20 864 to 22 030 cm^{-1} at 18 K produced exponential emission decay curves from the $^3P_0$ state with a decay constant of 2150 s^{-1} (Fig. 4). As the temperature is raised the decay constant increases monotonically becoming 7520 s^{-1} at 293 K. Excitation at 20 670 cm^{-1} (into a region of weak absorption *ca.* 70 cm^{-1} to high energy of the $^3P_0$ electronic origin), at 21 650 cm^{-1} (into a region of weak absorption between the $^3P_1$ and $^3I_6$ states), and 22 254 cm^{-1} (i.e. into a region of weak absorption between the $^3I_6$ and $^3P_2$ states) at 18 K produces markedly different decay curves characterised by a prominent very fast relaxation at short times and a long exponential tail corresponding to a decay constant of 2380 s^{-1} i.e. slightly faster than the decay constant when the excitation is into the stronger absorption bands (Figs. 4, 5). The initial decay of the fast process (or processes) during the first few microseconds corresponds to a rate constant of about 10^6 s^{-1}, but the decay kinetics of this process are themselves strongly non-exponential so that after 20 μs the decay constant is about 5×10^4 s^{-1}. The overall shapes of these three curves are similar but not identical. Moreover there are some small differences depending of the luminescence transition monitored. On increasing the temperature, this fast process and the differences in the slow decay gradually vanish and not present in the 298 K curves.

These experiments were repeated using a sample of composition $Cs_2NaY_{0.9997}Pr_{0.0003}Cl_6$, the results were closely similar but the poorer signal to noise ratio achieved prevented any precise comparisons of the relative intensities of the fast and slow processes in the two crystals.

5. Discussion

The behaviour of the $x = 0.01$ crystals is entirely consistent with our shell model [1]. Within this model the acceptors are collected in individual shells labelled as $n = 1$ (nearest donor–acceptor neighbour) at a distance R_1, $n = 2$ (next nearest neighbour) at a distance R_2 etc. The maximum number of ions in the n-th shell is N_n, these integers are determined by the symmetry of the crystal lattice. When $x < 1$, not all the available N_n sites will be occupied by an acceptor and we introduce an occupancy integer r_n for each shell where $0 < r_n < N_n$.

For a large number of Ln^{3+} ions randomly distributed in a crystal lattice of composition $Cs_2NaY_{1-x}Ln_xCl_6$ it is necessary to average over all the r_n occupancy numbers. In the case of a particular Ln^{3+} ion, the statistical probability of a specific shell n surrounding having r_n sites occupied by a Ln^{3+} ion and $N_r - r_n$ sites occupied by Y^{3+} ions may be written

$$O_{r_n}^{N_n}(x) = \frac{N_n!}{(N_n - r_n)!r_n!}(1-x)^{N_n - r_n}x^{r_n}. \tag{1}$$

The time evolution of an excited state involved in cross-relaxation by an electric dipole–electric dipole mechanism is given by

$$I(t) = I(0)\exp(-kt)\prod_{n}^{\text{all shells}}\sum_{r_n}^{N_n} O_{r_n}^{N_n}(x)\exp\left[-r_n\left(\frac{R_1}{R_n}\right)^6 k^{\text{CR}}t\right]. \tag{2}$$

Here k is the sum of all the rate constants describing the decay processes of the isolated excited ion and k^{CR} is the energy transfer rate to a single ion at the position of the nearest neighbour acceptor.

For the elpasolite lattice, the successive terms in the product rapidly approach unity because of the factor R_n^{-6} in the exponential term. $N_1 = 12$ and therefore $O_{r_1}^{12}(0.01) = 0.886, 0.107, 0.005$ for $r_1 = 0, 1, 2$ and the contributions from the other shells are smaller. The dominant terms in (2) for $x = 0.01$ are then

$$I(t) = I(0)\exp(-kt)\left[0.886 + 0.107\exp(-k^{CR}t) + 0.005\exp(-2k^{CR}t)\right]$$
$$\times\left[0.94 + 0.05\exp\left(-\frac{k^{CR}}{8}t\right) + 0.001\exp\left(-\frac{k^{CR}}{4}t\right)\right]$$
$$\times\left[0.78 + 0.19\exp\left(-\frac{k^{CR}}{27}t\right) + 0.02\exp\left(-\frac{2k^{CR}}{27}t\right)\right]. \quad (3)$$

For $x = 1$ only the $r_n = N_n$ terms contribute and the decay is exponential with a decay rate [1] of $k + 14.42k^{CR}$.

If $k \gg k^{CR}$ then, in the presence of Poisson distributed counting statistics and other minor sources of experimental uncertainty, this decay curve (3) cannot be experimentally distinguished from a single exponential with a decay constant slightly greater than k. However, for $k \ll k^{CR}$ the second term in the first square bracket may now be clearly separated from the first term and Eq. (3) then approximates to the sum of two exponentials with pre-exponential factors in the ratio of 8.3:1. At 20 K $k = 2110\ s^{-1}$ (see below) and the exponential decay rate for $x = 1$ is $9220\ s^{-1}$ so that $k^{CR} = 493\ s^{-1}$; this is entirely consistent with the experimental observation of a single exponential decay with $k \approx 2150\ s^{-1}$. However, at 293 K the exponential decay rate for $x = 1$ is about $10^6\ s^{-1}$ so that $k^{CR} = 70\,000\ s^{-1}$ and the exponential decay constant for $x = 0.001$ is $7300\ s^{-1}$ so we observe a bi-exponential decay. The shell model also accounts well for the experimental data over the whole concentration range $x = 0.01$ to 1 [1, 2].

This faster process in the decay curve of the $x = 0.001$ at 20 K is quite different from that in the $x = 0.01$ crystal in that its observation is excitation wavelength dependent and it is only observed at low temperatures. Since it is present at the lowest dilutions and the initial decay rate is much faster than in the $x = 0.01$ material it is not due to an interaction between Pr^{3+} ions (the occupancy factors are essentially unity for $r = 0$ and otherwise near zero). The similarity of the phenomena when excitation is just above the $^3P_0$ electronic origin and into the region between the $^1I_6$ and $^3P_2$ vibronic structure shows that it is not due to slow relaxation between the states in the 20 600 to 22 220 cm^{-1} region. The emission has a similar wave number dependence as that of the $PrCl_6^{3-}$ ion, and must involve a chemically similar species. We propose that this fast process is due to emission from $PrCl_6^{3-}$ ions perturbed by a nearby defect or impurity. The most likely impurity is water, possibly in association with an oxide ion impurity on a chloride site providing charge compensation. Indeed, absorption due to traces of water can be detected at 1500 and *ca.* 2800 cm^{-1} in the single crystal infrared absorption spectra. A similar explanation of the luminescence behaviour of $Cs_2NaEuCl_6$ has been given [7]. These perturbed sites absorb radiation outside the main absorption

bands of the unperturbed sites and may then be selectively excited in regions corresponding to little absorption of the unperturbed sites. Tanner [6] has reported the presence of defect sites in the absorption spectra of single crystals of this material. The energy gap between the $^3P_0$ and $^1D_2$ states can be bridged by two quanta of vibrational modes associated with the water. The very fast initial decay is due to Pr^{3+} ions close to water molecules, the slightly slower decays correspond to more distant water–Pr^{3+} interactions. The dipoles associated with the vibrational transitions of the water molecule are very much greater than that due to the vibronic transitions of a lanthanide ion so the quenching effect of a nearby water will be strong but some quenching will be detectable at rather large distances. The superposition of all these processes onto the slow decay of the very weakly and unperturbed sites will give a decay curve with the general shape of the Inokuti–Hirayama (III) model but differing in detail, this is what is observed experimentally. Extensive efforts to fit the data to the III model invariably gave meaningless parameter values.

The absence of the fast process at concentrations greater than $x = 0.01$ implies that the Pr^{3+} ions scavenge water molecules from the host lattice. The absence at high temperatures is probably due to line broadening in the excitation spectra together with an increase in the quenching efficiency of the waters nearest to a Pr^{3+} which reduces the emission intensity of those ions still further.

6. Conclusion

The initial fast process in the $^3P_0 \rightarrow {}^3H_4$ and $^3P_0 \rightarrow {}^3H_4$ luminescence decay curves of $Cs_2NaY_{0.999}Pr_{0.001}Cl_6$ observed is due to contamination of the sample with traces of water and not due to interactions between Pr^{3+} ions. Great care is necessary in the interpretation of decay curves in these materials, although measurement of the decay curves as a function of excitation wavelength is a useful guide to their reliability.

C.D.F. thanks The Royal Society for a travel grant to Chile. S.O.V. wishes to thank to The British Council and Fundacion Andes for the award of a Jack Ewer postdoctorial scholarship at the Laser Laboratory, Birkbeck College, University of London. The work in Chile has been supported from Grant DTI Q3670-9313 of the University of Chile and SI/93 from the Department of Basic Chemistry.

References

[1] C.D. Flint, S.O. Vasquez, *Chem. Phys. Lett.* **238**, 378 (1995).

[2] S.O. Vasquez, C.D. Flint, R. Sabry-Grant, *J. Appl. Spectrosc.* **62**, 213 (1995).

[3] T. Luxbacher, H.P. Fritzer, C.D. Flint, R. Sabry-Grant, *Chem. Phys. Lett.* **241**, 103 (1995).

[4] C.D. Flint, R. Sabry-Grant, *J. Appl. Spectrosc.* **62**, 154 (1995).

[5] T. Luxbacher, H.P. Fritzer, C.D. Flint, *J. Phys., Condens. Matter* **7**, 9683 (1995).

[6] P.A. Tanner, *Mol. Phys.* **57**, 697 (1982).

[7] M. Bettinelli, C.D. Flint, *J. Phys., Condens. Matter* **3**, 7053 (1991).